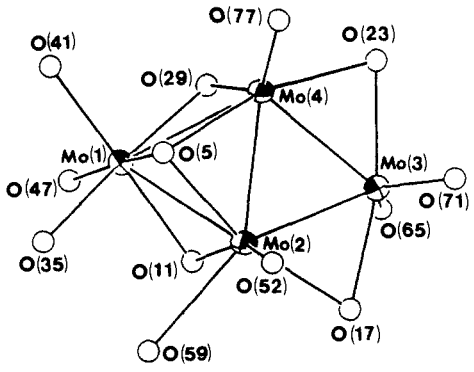

Figure 2. Ball-and-stick drawing of the central core of $Mo_4(OCH_2\text{-}c\text{-}Bu)_{12}(HOCH_2\text{-}c\text{-}Bu)$. The metal–metal distances are as follows (Å): Mo(1)–Mo(2) = 2.66 (1), Mo(1)–Mo(4) = 2.68 (1), Mo(2)–Mo(4) = 2.46 (1), Mo(3)–Mo(4) = 2.47 (1), Mo(2)–Mo(3) = 2.51 (1). The esd's are averaged for the two independent molecules in the unit cell.

cluster type we attempted single-crystal X-ray diffraction studies on IV, V, VIII, IX, X, and XI. Unfortunately, the crystals obtained only diffracted to small angles, and it was concluded that the structure consisted of hexagonal close-packed molecules with a molecular disorder. However, a suitable crystal of a derivative of XI was obtained with lower symmetry, and the single-crystal X-ray diffraction structure was solved.[8]

The structure obtained for this species is shown in Figure 2 which satisfies the molecular formula $[M_4(OR)_{12}(HOR)]$ where an extra molecule of alcohol is present and has destroyed the symmetry and packing of the $M_4(OR)_{12}$ compound. The structure consists of a butterfly arrangement of metal atoms with one triangular face capped with a triply bridging alkoxide ligand, and each edge is bridged by alkoxide ligands. Mo(2) possesses one terminal alkoxide ligand and is also coordinated to another oxygen atom at a distance of 2.33 Å, in the range we have previously observed for metal-to-alcohol oxygen distances.[9]

The preference for this structure over that of II is probably a result of the smaller steric requirement of the alkoxide ligands $O\text{-}CH_2R$ versus OR (same R) with the achievement of a greater number of M–O bonds and an octahedral coordination environment for Mo(1) providing a thermodynamic driving force.

Removal of the coordinated alcohol molecule from $Mo_4(OCH_2\text{-}c\text{-}Bu)_{12}(HOCH_2\text{-}c\text{-}Bu)$ would allow the structure of XI to be consistent with the NMR spectroscopic data obtained for the remaining members of this cluster class. In solution it is possible that the alkoxide ligands denoted by O(41), O(5), O(65), and O(71) lie on a mirror plane which also passes through molybdenum atoms (1) and (3). This leaves eight alkoxide ligands related in a pair-wise manner by the mirror plane, accounting for the observed integral ratios. In benzene-d_6 solution crystals of $Mo_4(OCH_2\text{-}c\text{-}Bu)_{12}(HOCH_2\text{-}c\text{-}Bu)$ dissociate the coordinated alcohol molecule, and XI exhibits similar NMR spectra to other members of this class.

The geometry of this new class of $M_4(OR)_{12}$ cluster is without precedent and taken together with the previous structures observed for $W_4(O\text{-}i\text{-}Pr)_{12}$[3] and $Mo_4X_4(O\text{-}i\text{-}Pr)_8$,[10] where X = Cl and Br, attests to the flexibility of metal–metal bonding in response to steric and electronic demands of the ancillary ligands.[11] Finally we note that this new class of $M_4(OR)_{12}$ compounds do *not* reversibly dissociate to form $M_2(OR)_6$ compounds, and coordinative unsaturation is maintained at three of the four metal sites. These are potentially available for substrate activation.[12]

Supplementary Material Available: A listing of fractional coordinates and bond distances and bond angles for the central Mo_4O_{13} moiety and stereoview of the molecules (9 pages). Ordering information is given on any current masthead page.

(7) A cryoscopic molecular weight determination on the compound $[Mo_4(OCH_2\text{-}i\text{-}Pr)_{12}]_n$ indicated that $n = 1$.

(8) Crystal data for $Mo_4(OCH_2\text{-}c\text{-}C_4H_8)_{12}(HOCH_2\text{-}c\text{-}C_4H_8)$ at −156 °C: $a = b = 19.952$ (7) Å, $c = 34.755$ (16) Å, $d_{calcd} = 1.432$ g cm^{-3}, $Z = 8$ and space group $P4_1$ (no. 76). Of 11 293 reflections collected, Mo Kα, $6° < 2\theta < 45°$, 9263 were unique, and the 7977 reflections having $F > 3.0\sigma(F)$ were used in the least-squares refinement. $R(F) = 0.058$ and $Rw(F) = 0.058$.

(9) Chisholm, M. H. *Polyhedron* **1983**, *2*, 681.

(10) Chisholm, M. H.; Errington, R. J.; Folting, K.; Huffman, J. C. *J. Am. Chem. Soc.* **1982**, *104*, 2025.

(11) Chloromolybdate ions, $Mo_4Cl_{12}^{3-}$, having 15 electrons available for M–M bonding have been found to adopt one of either rectangular or butterfly Mo_4 geometries in the solid state depending upon the nature of the counter cation: Aufdembrink, B. A.; McCarley, R. E. *J. Am. Chem. Soc.* **1986**, *108*, 2474.

(12) We thank the Department of Energy, Office of Basic Sciences, Chemistry Division for support of this work.

Synthesis of Bicyclic Keto Silanes by Tandem Rearrangement of Silylacetylenic Ketones

Andrew S. Kende,* Paul Hebeisen, and Ronald C. Newbold

Department of Chemistry, University of Rochester Rochester, New York 14627

Received December 11, 1987

In developing a general route to differentially functionalized fused bicyclic systems we have explored the thermal rearrangement of cycloalkanones bearing an ω-silylacetylenic chain β to the carbonyl group. We now report that the prototype system **1a** undergoes a novel sequence of tandem rearrangements leading to the bicyclic dienol silane **2a** and that by appropriate structural modifications we can alter the reaction pathway to provide a new, high-yield synthesis of bicyclic allylsilane ketones.

When ketone **1a**[1] was held at 300 °C (neat, 2 h), the major product (60–65% yield) was a carbonyl-free isomer[2] showing by 300 MHz ^{1}H NMR an allylic CH_3 (3 H, δ 1.96, s), an olefinic proton at δ 4.93 (1 H, m), and $OSiMe_3$ at δ 0.22 (9 H, s). Since this product could be quantitatively hydrolyzed in wet tetrahydrofuran to the known conjugated ketone **3a**[3] and dehydrosilylated ($Pd(OAc)_2$, MeCN, room temperature, 14 h, 59% yield)[4] to the cross-conjugated dienone **4a**,[5] its structure was established as the dienol silane **2a**.[2]

The unexpected formation of dienol silane **2a** from acetylene **1a** could be rationalized by a multiple rearrangement sequence proceeding through initial enolization of **1a** to **5a**, Conia cyclization[6,7] to vinylsilane **6a**, prototropic double bond migration to conjugated enone **7**, followed by Casey rearrangement[8] of silicon to oxygen giving **8**, and a final prototropic rearrangement to the more stable diene tautomer **2a** (Scheme I).

If the indicated mechanism is correct, placement of an alkyl group at C-2 in **1**, leading to **6b**, would prevent isomerization to **7** and arrest the reaction at the vinylsilane stage. However, when

(1) Ketones **1** were synthesized by conjugate addition of the appropriate ω-trimethylsilylalkynylmagnesium chloride (THF, 0.45 equiv of CuI) to the corresponding conjugated enone, as described by House and Fischer (House, H. O.; Fischer, W. F. *J. Org. Chem.* **1969**, *34*, 3615). All ketones **1** were fully characterized by IR, NMR, combustion analysis, and MS and distilled before use. The α-methyl ketones **1b–e** were used as cis/trans mixtures. Ketone **1a**: IR (film) 2175, 1710 cm^{-1}; ^{1}H NMR (300 MHz, $CDCl_3$) δ 2.28 (3 H, m), 2.16 (2 H, t), 1.93 (4 H, m), 1.56 (1 H, m), 1.47 (2 H, dt), 1.27 (1 H, m), 0.04 (9 H, s); MS, 222 (M^+). Anal. Calcd for $C_{13}H_{22}OSi$: C, 70.21; H, 9.97. Found: C, 70.32; H, 9.99.

(2) Enolsilane **2a**: ^{1}H NMR (300 MHz, $CDCl_3$, partial) δ 4.89 (1 H, m), 1.96 (3 H, s), 0.22 (9 H, s); IR no C=O; MS, calcd for $C_{13}H_{22}OSi$ 222.1440, found 222.1405; UV (MeOH) λ_{max} 252 nm, ϵ 11 927.

(3) Weisbuch, F.; Yamagami, C.; Dona, G. *J. Org. Chem.* **1972**, *37*, 4334.

(4) Ito, Y.; Hirao, T.; Saegusa, T. *J. Org. Chem.* **1978**, *43*, 1011.

(5) Dienone **4a**: ^{1}H NMR (400 MHz, $CDCl_3$, partial) δ 6.70 (1 H, ddd, J = 10, 7, 3), 5.80 (1 H, dd, J = 10, 3), 2.10 (3 H, s).

(6) For a review, see: Conia, J. M.; LePerchec, P. *Synthesis* **1975**, 1.

(7) Thermal cyclizations of simple acetylenic ketones have been reported by Agosta and Wolff (Agosta, W. C.; Wolff, S. *J. Org. Chem.* **1975**, *40*, 1699) and by Drouin et al. (Drouin, J.; Leyendecker, F.; Conia, J. M. *Tetrahedron Lett.* **1975**, 4053). Mercuric ion-catalyzed cyclizations of ϵ-acetylenic ketones are known, cf.: Boaventura, M. A.; Drouin, J.; Conia, J. M. *Synthesis* **1983**, 801.

(8) Casey, C. P.; Jones, C. R.; Tukada, H. *J. Org. Chem.* **1981**, *46*, 2089.

0002-7863/88/1510-3315$01.50/0

Scheme I

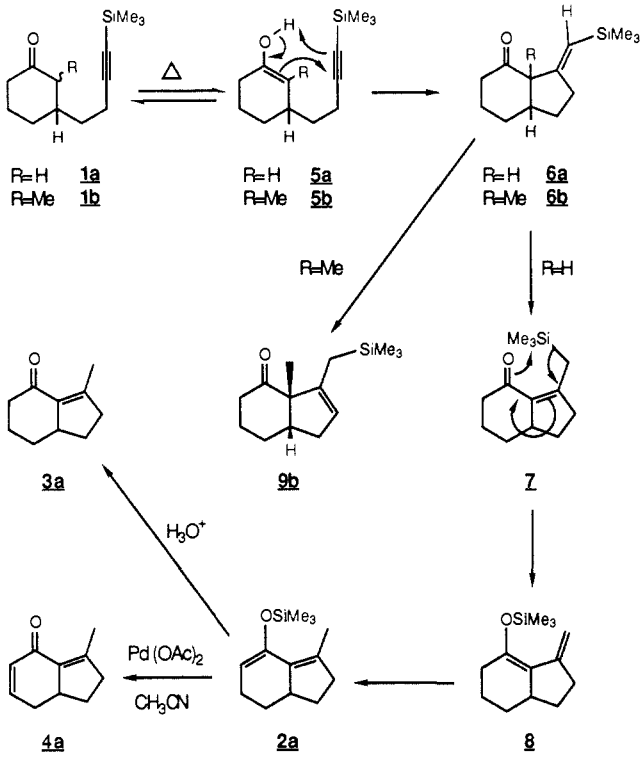

Table I

reactant	conditions	product	yield[a] (%)
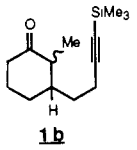 1b	285 °C, 1.5 h, neat	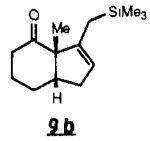 9b	75
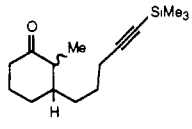 1c	285 °C, 48 h, neat	 9c	65[b]
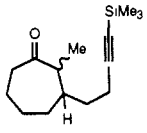 1d	285 °C, 2 h, neat	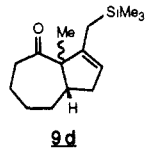 9d	62[c]
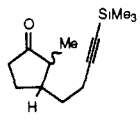 1e	285 °C, 1.5 h, neat	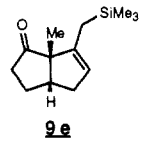 9e	91

[a] Isolated yield reported. [b] Approximately 12:1 cis/trans ring junction (NMR). [c] Approximately 6:1 ring junction stereochemistry ratio by NMR.

the methyl-substituted ketone **1b** (cis/trans mixture)[9] was held at 280 °C (neat, 1.5 h), an unexpected product was again isolated in 75% yield. Careful 300 MHz ^{1}H NMR studies in C_6D_6 showed this to be the *allylsilane* **9b**.[10] Particularly diagnostic were the characteristic[11] upfield CH_2SiMe_3 signals as an AB quartet centered at δ 1.48 with J = 15 Hz, only weakly perturbed by small (~1 Hz) long-range couplings to the cyclopentene ring protons. We have found that this cyclization is general and proceeds in high yield for a series of silylacetylenic ketones (Table I). Ring junction stereochemistries for **9b** and **9e** are assumed cis, and that for the major product from **1c** was established as cis by its conversion (1.3 equiv of mCPBA, 2 equiv of $NaHCO_3$, CH_2Cl_2, room temperature, then crystallized from $CHCl_3$–hexane) to the hemiketal **10**, for which an X-ray single-crystal structure determination has been obtained.[12]

Scheme II

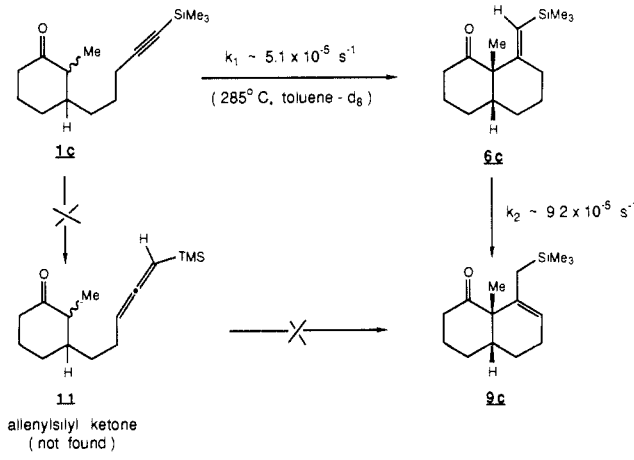

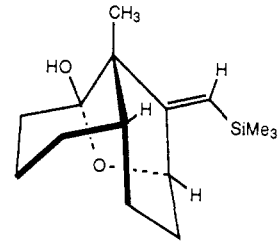

10

Our synthesis of allylsilanes **9** rather than vinylsilanes **6** could reflect arrival at a thermodynamic sink[13] or possibly kinetic product derived from Conia cyclization of an allenylsilyl ketone such as **11**. Direct evidence for the former alternative was obtained by quantitative monitoring of the thermal rearrangement of **1c** at 285 °C in toluene-d_8 with 300 MHz ^{1}H NMR. During the reaction ($\tau_{1/2}$ = 3.5 h) the appearance of an intermediate identified as **6c**[14] could be measured, reaching a maximum of 35% (based on starting **1c**) at 4.0 h. From our kinetic analysis we conclude that **1c** undergoes first-order conversion to **6c** (Scheme II) and that **6c** undergoes subsequent prototropic isomerization to **9c**,[15] the thermodynamic product.

Thermal isomerizations of silylacetylenic ketones **1** are shown to proceed within a tandem rearrangement manifold which may be diverted to fused bicyclic allylsilane ketones in high preparative

(9) Ketone **1b**: Calcd for $C_{14}H_{24}OSi$: C, 71.12; H, 10.23; Si, 11.88. Found: C, 71.56; H, 10.32; Si, 11.99.

(10) Allylsilane **9b**: ^{1}H NMR (300 MHz, C_6D_6) δ 5.26 (1 H, br s), 2.15 (2 H, m), 1.96 (1 H, m), 1.88 (1 H, br dt), 1.57 (2 H, m), 1.48 (2 H, AB q, J = 15), 1.27 (3 H, s), 1.14 (3 H, m), −0.02 (9 H, s). Anal. Calcd for $C_{14}H_{24}OSi$: C, 71.12; H, 10.23. Found: C, 70.86; H, 10.36.

(11) E.g.: Fleming, I.; Patterson, I. *Synthesis* **1979**, 446.

(12) We thank Dr. J. Gougoutas and M. Malley (Squibb Institute for Medical Research) for carrying out the X-ray determination of the structure **10**.

(13) Rhodium(I)-catalyzed prototropic isomerizations of acyclic unsaturated silanes have been recently reported by Matsuda et al. (Matsuda, I.; Kato, T.; Sato, S.; Izumi, Y. *Tetrahedron Lett.* **1986**, *27*, 5747). These data strongly suggest that acyclic allylsilanes are more stable than vinylsilanes, in contrast to the conclusions of Slutsky and Kwart (Slutsky, J.; Kwart, H. *J. Am. Chem. Soc.* **1973**, *95*, 8678).

(14) Vinylsilane **6**: ^{1}H NMR (300 MHz, $CDCl_3$, partial) δ 4.85 (1 H, s), 1.30 (3 H s), 0.06 (9 H, s).

(15) Allylsilane **9c**: ^{1}H NMR (300 MHz, $CDCl_3$) δ 5.39 (1 H, br s), 2.32 (1 H, dt), 2.22 (2 H, m), 2.00 (2 H, m), 1.78 (3 H, m), 1.52 (3 H, m), 1.24 (2 H, m), 1.15 (3 H, s), 0.00 (9 H, s); ^{13}C NMR ($CDCl_3$, partial) δ 215.4 (C=O), 135.05 (C-8), 121.5 (C-9). Anal. Calcd for $C_{15}H_{26}OSi$: C, 71.93; H, 10.46. Found: C, 72.22; H, 10.35.

yields. The applications of this simple reaction for the preparation of spirocyclic and bridged ketosilanes, and for hirsutane synthesis, are in progress.[16]

Registry No. 1a, 113893-24-6; **1b**, 113893-25-7; **1c**, 113893-26-8; **1d**, 113893-27-9; **1e**, 113893-28-0; **2a**, 113893-29-1; **3a**, 40730-45-8; **4a**, 113893-30-4; **6c**, 113893-40-6; **9b**, 113893-31-5; *cis*-**9c**, 113893-32-6; *trans*-**9c**, 113893-33-7; *cis*-**9d**, 113893-34-8; *trans*-**9d**, 113893-35-9; **9e**, 113893-36-0; **10**, 113893-37-1; 2-methyl-2-cyclohexen-1-one, 1121-18-2; 2-methyl-2-cycloheptenone-1-one, 65371-57-5; 2-methyl-2-cyclopenten-1-one, 1120-73-6; ω-trimethylsilylbutynylmagnesium chloride, 113893-38-2; 2-cyclohexen-1-one, 930-68-7; ω-trimethylsilylpentynylmagnesium chloride, 113893-39-3.

(16) Partial support of this research by Grant CA-18846, awarded by the National Cancer Institute, USPHS, is gratefully acknowledged. We thank Dr. Ronald Valente for preparation of certain intermediates used in this study.

Properties of the Fe(II)–Fe(III) Derivative of Red Kidney Bean Purple Phosphatase. Evidence for a Binuclear Zn–Fe Center in the Native Enzyme

Jennifer L. Beck, John de Jersey, and Burt Zerner*

Department of Biochemistry, University of Queensland St. Lucia, Queensland, Australia 4067

Michael P. Hendrich and Peter G. Debrunner*

Department of Physics, University of Illinois Urbana, Illinois 61801

Received December 15, 1987

Purple phosphatases from pig allantoic fluid[1] and beef spleen represent a class of metallohydrolases which contain a binuclear iron center.[2-5] These enzymes exist in two redox states, a pink, catalytically active Fe(II)–Fe(III) form and a purple catalytically inactive Fe(III)–Fe(III) form. EPR spectroscopy and magnetic susceptibility measurements[4,6] have shown that the iron atoms are antiferromagnetically coupled. The oxidized Fe(III)–Fe(III) forms of these enzymes are EPR silent, whereas the reduced forms have a characteristic low-temperature EPR spectrum with a rhombic g tensor, g = (1.94, 1.73, 1.57), corresponding to one unpaired electron per binuclear center.[4,5,7] Recently, we reported the purification and characterization of a purple phosphatase from red kidney bean which contains one atom of iron and one of zinc per subunit of ~60 kDa.[8] Further, we have shown that it is possible to prepare a catalytically active Fe(II)–Fe(III) form of the red kidney bean enzyme.[9]

In this report, we compare the low-temperature EPR spectra of the native Zn–Fe form **1** and the Fe(II)–Fe(III) derivative **2** of red kidney bean purple phosphatase with that of the Fe(II)–Fe(III) form of pig allantoic fluid acid phosphatase (**3**). The spectra of **2** and **3** are very similar, showing that **2** and, therefore by inference, the native Zn–Fe red kidney bean purple phosphatase (**1**) contain a binuclear complex.

A sample of **2** was prepared by treatment of a solution of the native enzyme in 0.1 M acetate buffer, pH 4.9, 0.5 M in NaCl, with ferrous ammonium sulfate and 2-mercaptoethanol ($[E]_0$ = 69 μM; $[Fe^{2+}]$ = 85.1 mM; [2-mercaptoethanol] = 136 mM) for 40 h at 25 °C. The enzyme was then separated from the other reagents by passage through a column of Sephadex G-25 equilibrated in the same buffer and concentrated by ultrafiltration. The enzyme sample so prepared (23.4 mg/mL; 0.39 mM in 60-kDa subunits) had a specific activity of 515 $U \cdot ml^{-1} \cdot A_{280}^{-1}$ in the standard assay at pH 4.9 with *p*-nitrophenyl phosphate as substrate and contained 1.92 Fe atoms and 0.24 Zn atoms per subunit. Treatment of an aliquot of this sample with 11 mM H_2O_2 for 2 min at 25 °C resulted in loss of 90% of the activity, showing that ≤10% of the activity was due to residual native (Zn–Fe) enzyme which is not inactivated by H_2O_2.[9,10]

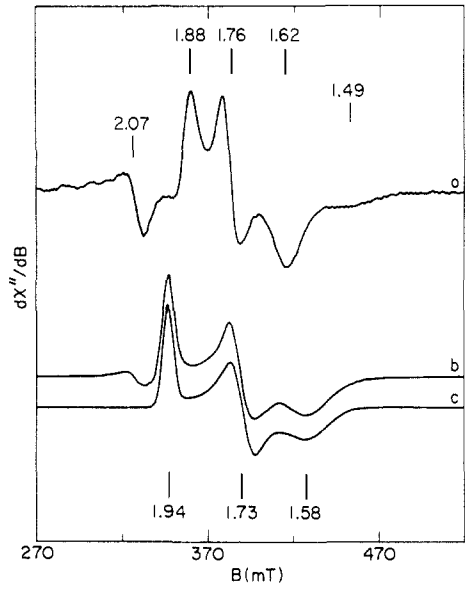

Figure 1. EPR spectra of the Fe(II)–Fe(III) derivative of (a) red kidney bean purple phosphatase (**2**) and (b) the reduced form of pig allantoic fluid acid phosphatase (**3**) at 4 K. The simulation (c) is based on an effective spin $S = 1/2$ Hamiltonian with $\tilde{g}$ = (1.94, 1.73, 1.58) and an anisotropic, Gaussian line width model with $\tilde{\sigma}$ = (7, 13, 27) mT. Spectral conditions: microwaves 9.447 GHz at 0.2 mW; 100 kHz modulation at 2 mT_{pp}; dB/dt = 0.6 mT/s.

Figure 1a shows the EPR spectrum at 4 K of the sample of **2** described above, together with the spectrum of a sample of the reduced form of pig allantoic fluid acid phosphatase (**3**; 0.53 mM) run under the same conditions (Figure 1b). The spectra shown in Figure 1 are clearly very similar, indicating that they arise from closely related metal ion complexes. Apart from a Cu(II) signal with $g_\perp \sim 2.06$ the main features of the spectra have g values $g < 2$ and are thus characteristic of an antiferromagnetically coupled pair of high-spin ferrous and ferric ions with zero-field splittings comparable to the exchange interaction.[11] The differences between the EPR signals of **2** and **3** are significant, however, and indicate differences in the structure of the complex. While we can simulate the spectrum of the pig enzyme with the effective g tensor and anisotropic Gaussian line width specified in the figure caption, spectrum 1a cannot be simulated by the same model. We conclude that the Fe(II)–Fe(III) signal of the bean enzyme is a superposition of at least two components, a view that is corroborated by the extra broad dip near g = 1.49. In this context, Averill et al.[12] have shown that the analogous EPR signal of the beef spleen enzyme is sensitive to changes in pH.

Figure 2 shows the EPR spectrum of a sample of native (Zn–Fe) red kidney bean phosphatase (**1**; 0.44 mM; specific activity 334 $U \cdot mL^{-1} \cdot A_{280}^{-1}$) at 4 K. The native Zn–Fe red kidney bean

(1) Pig allantoic fluid purple acid phosphatase has also been called uteroferrin, although there is little evidence in support of the implied function: Roberts, R. M.; Bazer, F. W. *BioEssays* **1984**, *1*, 8-11.
(2) Campbell, H. D.; Dionysius, D. A.; Keough, D. T.; Wilson, B. E.; de Jersey, J.; Zerner, B. *Biochem. Biophys. Res. Commun.* **1978**, *82*, 615-620.
(3) Debrunner, P. G.; Hendrich, M. P.; de Jersey, J.; Keough, D. T.; Sage, J. T.; Zerner, B. *Biochim. Biophys. Acta* **1983**, *745*, 103-106.
(4) Davis, J. C.; Averill, B. A. *Proc. Natl. Acad. Sci. U.S.A.* **1982**, *79*, 4623-4627.
(5) Antanaitis, B. C.; Aisen, P. *Adv. Inorg. Biochem.* **1983**, *5*, 111-136.
(6) Sinn, E.; O'Connor, C. J.; de Jersey, J.; Zerner, B. *Inorg. Chim. Acta Bioinorg. Art. Lett.* **1983**, *78*, 13-15.
(7) Roberts, R. M.; Bazer, F. W. *J. Biol. Chem.* **1980**, *255*, 11204-11209.
(8) Beck, J. L.; McConachie, L. M.; Summors, A. C.; Arnold, W. N.; de Jersey, J.; Zerner, B. *Biochim. Biophys. Acta* **1986**, *869*, 61-68.
(9) Beck, J. L.; de Jersey, J.; Zerner, B. *Abstracts, 13th Int. Congress Biochem., Amsterdam* **1985**, 66.
(10) Beck, J. L.; Keough, D. T.; de Jersey, J.; Zerner, B. *Biochim. Biophys. Acta* **1984**, *791*, 357-363.
(11) Sage, J. T.; Debrunner, P. G. *Hyperfine Interactions* **1986**, *29*, 1399-1402.
(12) Averill, B. A.; Davis, J. C.; Burman, S.; Zirino, T.; Sanders-Loehr, J.; Loehr, T. M.; Sage, T. J.; Debrunner, P. G. *J. Am. Chem. Soc.* **1987**, *109*, 3760-3767.

0002-7863/88/1510-3317$01.50/0